MoM-GEC Analysis of Fraunhofer-Region Characteristics over Rectangular Aperture

Imen Khadhraoui[1(✉)], Taha Ben Salah[2], and Taoufik Aguili[1]

[1] Communications Systems Laboratory (SysCom), National Engineering School of Tunis (ENIT), University of Tunis El Manar, Tunis, Tunisia
imenk1986@gmail.com, taoufik.aguili@gmail.com

[2] Networked Objects Control and Communication Systems (NOCCS), National Engineering School of Sousse (ENISo), University of Sousse, Sousse, Tunisia
taha.bensalah@gmail.com

Abstract. In this paper, a determination of radiation characteristics is performed using rectangular aperture antenna theory and transverse electric field calculation with method of moments and generalized equivalent circuit MoM-GEC for a rectangular patch antenna contained in an open-ended waveguide. This study is based on aperture antenna theory and field equivalence principle applied to the two-dimensional Fourier transform integrals over the aperture. We consider Fraunhofer-zone characteristics in terms of radiation pattern and directivity computed over an aperture through an assumed perfectly conducting screen. Results show an acceptable agreement between computed and simulated radiation data in E and H planes.

Keywords: Aperture antenna · Radiation characteristics
MoM-GEC analysis · Planar circuit

1 Introduction

Antenna radiation characteristics are a fundamental key performances in EM analysis. The determination of radiated properties is based on radiation analysis over apertures. In this study, we are interested in radiation analysis over a rectangular aperture antenna. Structure analysis is evaluated in terms of radiation pattern and directivity using rigorous formulation based on MoM-GEC method (Galerkin implementation in spatial domain of method of moments) and comparing with commercial simulation software CST MWS. Such analysis is intended to infer full 3D calculation of electromagnetic fields while benefiting of MoM simplification that helps determination of unknowns at the very discontinuity plane and hence bringing back 3D spatial problem to 2D spatial problem.

The main aim of this study is to perform radiation characteristics over rectangular aperture. In fact, Fraunhofer zone is closely related to far-zone approximation technique. Hence, this work describes a brief formulation to determine

V. Sucasas et al. (Eds.): BROADNETS 2018, LNICST 263, pp. 279–288, 2019.
https://doi.org/10.1007/978-3-030-05195-2_27

radiation characteristics of a planar circuit based on MoM-GEC method. A set of spatial expressions of Galerkin method are used in this work to investigate electromagnetic performances to conclude thereafter about far-zone characteristics in terms of far field, radiation pattern and directivity.

To outline this paper, our description is organized into four sections. Section 2 is dedicated to introduce few works about radiation approaches over different aperture types. In Sects. 3 and 4, the studied structure and the numerical method analysis is described. In the Sect. 5, an investigation of computed radiation data is presented and discussed.

2 Related Work

There are several types of aperture antennas such as rectangular apertures, circular apertures, open-ended waveguides. Radiation apertures are based on field equivalence principle to express aperture fields by equivalent electric and magnetic surface currents. At Fraunhofer-zone, by the knowledge of the fields over the aperture of the antenna, aperture fields are considered the sources of radiation (Huygens-Fresnel principle).

In [1], a parabolic circular-ended taper is studied to find out maximum power which is computed from circular cophasal aperture based on field equivalence principle formula. A normalized power flux density on the axis of the aperture is also computed in order to enhance factors of different aperture field distributions within various aperture sizes.

Open-ended waveguide is one of radiation aperture types studied in the literature [2]. In [3], field radiated from rectangular open-ended waveguide is determined based on gain correction factor approach of Polk. The open-ended waveguide is excited with TE10 mode and the gain pattern is computed over the open-ended waveguide at Fresnel-zone.

In [4], an approach for calculating the far zone pattern from near field measurements is described. Near field data is utilized to determine far field based on two-dimensional Fourier transform over the aperture of the antenna. A replacement of integrals by a summation over constant increments in X and Y is done to compute far field from a measured near field.

In [5], an integral solution based on vector potentials to determine far field patterns is presented. In, fact, moments method-based is applied to analyze microstrip square patch to evaluate far field results. MoM results are computed in terms of radiation pattern in H and E planes based on Green's functions defined in an assumed infinite substrate to describe a square patch excited with a dipole (coaxial port). A comparison is presented in [5] between results computed with transmission line model, measured data and results obtained by MoM analysis with two types of base functions. Since results are computed with an assumed finite substrate, a negligible effect on radiated fields in H-plane however is investigated and a poor agreement is noted with all compared cases in the E-plane results. In this context, an investigation of finite substrate effect on electric field is studied preceding determination of radiation performances in this work.

3 Studied Structure

The studied structure is a planar circuit: the radiated element is rectangular patch. In this section a description of the studied structure and parameters are given in addition to a concise formulation for radiated properties determination.

3.1 Structure Parameters

The geometry of the structure is shown in Fig. 1 [6]. A microstip rectangular patch antenna acts as radiated element. It is contained in a bounded domain and is placed on short circuited substrate (loss free, 2.2 dielectric constant). The ground plane, the patch and the feed line are designed as PEC. The antenna is contained in an open-ended waveguide (four electric sidewalls EEEE) with short-circuited bottom side (z-axis). Excitation source is considered as constant planar pulse function.

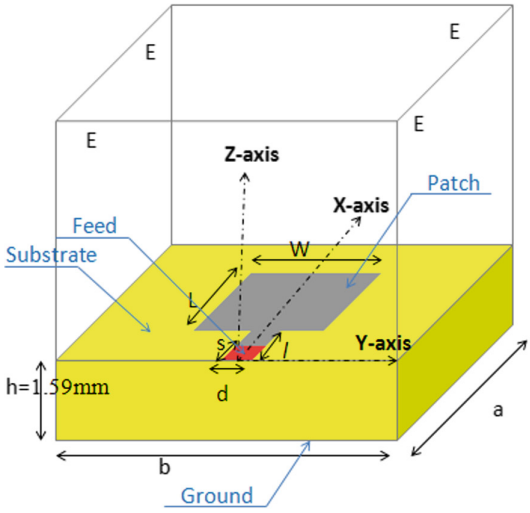

	Length (mm) (along x axis)	Width (mm) (along y axis)
Source	0.786 (s)	2.812 (d)
Feed line	5.690 (l)	2.812 (d)
Patch antenna	22.760 (L)	5.989 (W)
Dielectric substrate	100.567 (a)	45 (b)
Ground plane	100.567 (a)	30 (b)

Fig. 1. Studied structure.

3.2 MoM-GEC Formulation

This paper's approach is based on MoM-GEC formulation as a first step of modeling, so that a characterization of surface E and Js fields are deduced. The second step relies on application of aperture theory to figure out Fraunhofer-zone properties. Numerical formulation is expressed with Galerkin implementation of moments method [7] in spatial domain combined with generalized equivalent

circuit MoM-GEC [8]. The equivalent circuit associated to the studied structure is made respecting all electromagnetic boundary conditions (Fig. 2), where:

- E0 is chosen as planar voltage source.
- Js is the surface current (unknown).
- Zsup, Zinf are respectively matched load impedance operator and short circuited impedance operator.
- E is the transverse electric field (unknown).

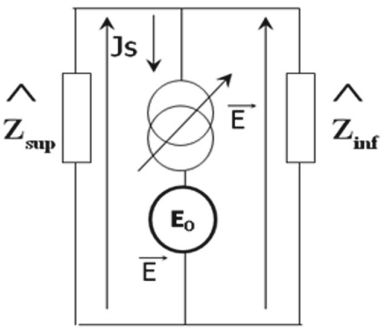

Fig. 2. Equivalent circuit of the studied structure.

Referring to the equivalent circuit, Eq. 1 is used to determine the two unknowns Js and E.

$$\begin{bmatrix} E \\ Js \end{bmatrix} = \begin{bmatrix} 1 & \hat{Z} \\ 0 & 1 \end{bmatrix} \begin{bmatrix} E_0 \\ J_0 \end{bmatrix} \tag{1}$$

$$(E - E_0) = \hat{Z} Js \tag{2}$$

The current J_s is discretized over test functions g_i (Eq. 3).

$$J_s = \sum_i x_i g_i \tag{3}$$

By replacing J_s, the Eq. 2 becomes:

$$\langle g_j, E - E_0 \rangle = \langle g_j, \hat{Z} \sum_i x_i g_i \rangle \tag{4}$$

The second projection on J_s (Galerkin application) gives Eq. 5:

$$\begin{bmatrix} \langle g_1, E_0 \rangle \\ \dots \\ \langle g_j, E_0 \rangle \\ \dots \\ \langle g_n, E_0 \rangle \end{bmatrix} = \begin{bmatrix} \langle g_1, \hat{Z} g_1 \rangle & \dots & \langle g_1, \hat{Z} g_n \rangle \\ \dots & \langle g_j, \hat{Z} g_i \rangle & \dots \\ \langle g_n, \hat{Z} g_1 \rangle & \dots & \langle g_n, \hat{Z} g_n \rangle \end{bmatrix} \begin{bmatrix} x_1 \\ \dots \\ x_i \\ \dots \\ x_n \end{bmatrix} \tag{5}$$

Consequently, the MoM-GEC matrix equation is expressed by:

$$B = AX$$

Where: A: Impedance matrix, B: Excitation column vector and X: Unknown coefficients vector.

So, X is evaluated by matrix inversion. Localized test functions are closely related to the current distribution on the metal. Test functions are set to bi-dimensional overlapping rooftops expressed in two sub-domains: the feed line sub-domain and the patch sub-domain. In the feed line sub-domain: $dLine = [0, l][-d/2, d/2]$, Eq. 6 is expressed as following:

$$gp_1(x, y) = \begin{cases} N_1(x - (p-1)\Delta l) & \text{in } dA \\ N_2(-x + (p+1)\Delta l) & \text{in } dD \end{cases} \tag{6}$$

where: $dA = [(p-1)\Delta l, p\Delta l][-d/2, d/2]$; $dD = [p\Delta l, (p+1)\Delta l][-d/2, d/2]$

In patch sub-domain $dPatch = [l, l + L][-W/2, W/2]$, test functions are defined (Eq. 7):

$$gp_2(x, y) = \begin{cases} N_1'(X - (p-1)\Delta l + l) & \text{in } dA' \\ N_2'(-x + (p+1)\Delta l + l) & \text{in } dD' \end{cases} \tag{7}$$

where: $dA' = [(p-1)\Delta l + l, p\Delta l + l][-W/2, W/2]$; $dD' = [p\Delta l + l, (p+1)\Delta l + l][-W/2, W/2]$

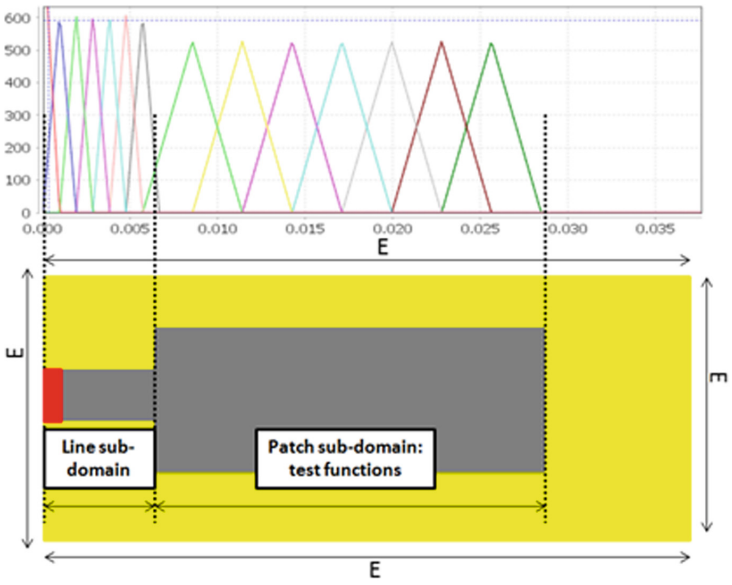

Fig. 3. One-dimensional plot of test functions rooftop type.

Test functions are normalized by factors $N1$, $N2$, $N'1$ and $N'2$. A representation of rooftops plot is given in Fig. 3. According to this formulation, the electric field E is expressed as Eq. (8) in Cartesian coordinates x and y.

$$E(x,y) = \sum_{mn} \sum_{pq} X_p z_{mn} \langle g_{pq}, f_{mn} \rangle f_{mn}(x,y) \tag{8}$$

The expression of the impedance operator is set according to homogeneous mode functions f_{mn} (electric and magnetic transverse TE and TM) of the waveguide mode impedances z_{mn}. MoM-GEC-based implementation leads to a computation of transverse E field. In the second step, we describe the application of aperture theory witch utilizes the computed electric field.

3.3 Aperture Theory Application

Referring to Huygens-Fresnel principle, E field becomes the source of radiation at the aperture. Radiation over aperture theory begins with the expression of Helmholtz solutions of Maxwell equations [9]. Solutions are obtained in terms of respectively electric and magnetic vector potentials. The application of field equivalence principle [9–11] expresses J_s and M_s, respectively electric and magnetic surface current densities, as functions of tangential electric and magnetic fields (Eqs. 9 and 10).

$$J_s = \hat{n} \times H_a \tag{9}$$

$$M_s = -\hat{n} \times E_a \tag{10}$$

We consider the rectangular aperture mounted in perfectly conducting screen at xy-plane. With the help of image theory principle [9], only magnetic current based on electric field prevails (Eq. 10). Consequently, the case of aperture over PEC entails a simplification of expressions describing radiated fields. Over PEC aperture, expressions of radiated field components are written as:

$$E_\theta = 2jk \frac{e^{-jkr}}{4\pi r} (f_x \cos(\phi) + f_y \sin(\phi)) \tag{11}$$

$$E_\phi = 2jk \frac{e^{-jkr}}{4\pi r} (\cos(\theta)(f_x \sin(\phi) + f_y \cos(\phi))) \tag{12}$$

Based on Fourier transform integrals over Cartesian aperture, f is expressed as:

$$f(\theta,\phi) = \int_{Aperture} E_a(x',y') e^{jk_x x' + jk_y y'} dx' dy' \tag{13}$$

In our case, the screen aperture is made in the plane XY, so the k_x and k_y are defined as: $k_x = kcos(\phi)sin(\theta)$, $k_y = ksin(\phi)sin(\theta)$.
Where $f(\theta,\phi)$ is function of tangential electric field expressed by means of MoM-GEC formulation.

4 Numerical Results

To describe all results related to the above formulation, a computer program Java/Scala-based is written. A convergence study is accomplished in terms of test and mode functions (226000 modes with 89 rooftops). Radiation characteristics are computed within the help of tangential electric field. Figure 4 illustrates electric field distribution calculated by MoM-GEC and CST MWS simulator. Plots show an agreement with physical boundary conditions. Electric field shows discontinuity of its X component at the patch right edge and has zero value on the metal. In our work, we are mainly interested in Fraunhofer-zone. Radiation data are computed in H and E planes: θ samples are set between $-\pi/2$ and $\pi/2$ where ϕ is constant $\phi = 0$, $\phi = \pi/2$, 30 samples are considered for θ and constant ϕ at the working frequency 4.79 GHz. Perpendicularly to the structure plane at z = 0, radiated field is computed at Fraunhofer zone (z = 1 m) based on Eq. 14.

$$E(\theta, \phi) = |E_\theta|^2 + |E_\phi|^2 \tag{14}$$

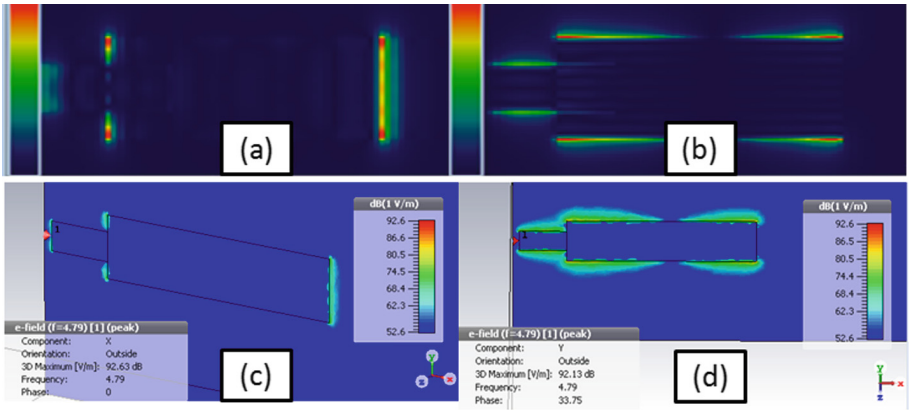

Fig. 4. Tangential E field components computed respectively with MoM-GEC and CST MWS: (a), (b): X and Y components of E field with MoM-GEC. (c), (d): X and Y components of E field with CST MWS.

Figure 5 depicts polar plot of radiated fields computed with MoM-GEC and simulated with CST MWS in H plane. Plots show an angle of aperture of about 67°. The non perfect agreement of the H-plane plots with CST MWS may be attributed to the shielding models in CST and MoM-GEC application. At the observation point r', based on radiated field components, radiation pattern is evaluated according to Eq. 15.

$$Poy(\theta, \phi) = \frac{r'^2}{2z_0}(|E_\theta|^2 + |E_\phi|^2) \tag{15}$$

where z_0 is the intrinsic impedance, r' is the distance of observation point. Figure (Fig. 6) shows polar plots of radiation pattern along the two planes with the two computation tools.

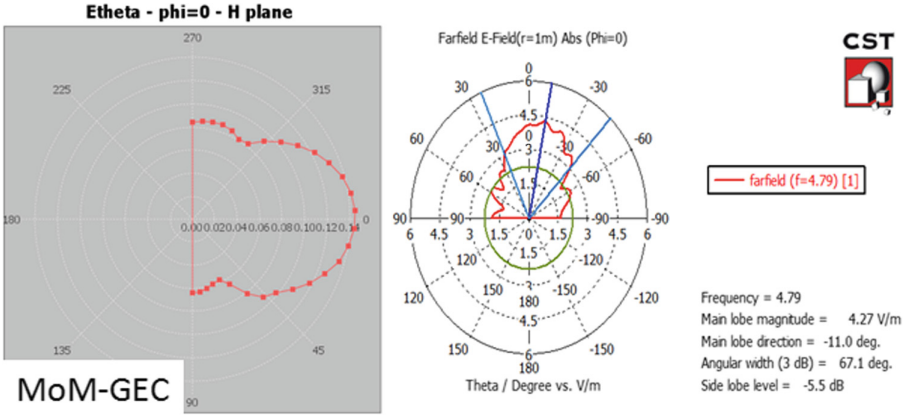

Fig. 5. Radiated Field H-plane polar plots (MoM-GEC computation and CST MWS simulation)

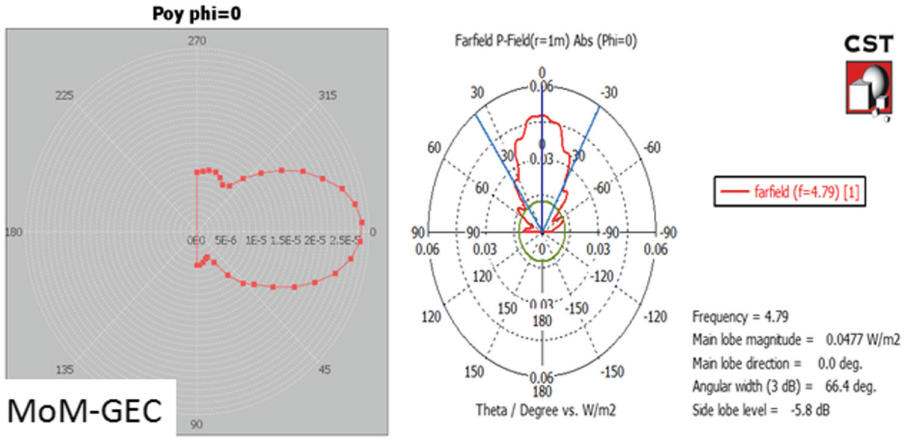

Fig. 6. Radiation pattern along H-plane polar plots (MoM-GEC computation vs CST MWS simulation).

The directivity is calculated by dividing radiation intensity by its average intensity (Eq. 16).

$$Dir = \frac{Poy(\theta, \phi)}{Poy(\theta, \phi)_{avg}} \tag{16}$$

Along the two principle planes, the directivity is computed using polar coordinates (ϕ is constant and θ is variable as mentioned above). Figures 7 and 8 show directivities obtained by both MoM-GEC-based formulation and simulation. By analyzing directivity intensity plots, main lobe value is about 5 dB obtained at the angle 0° producing an acceptable directivity level. Side lobe level is about −5.8 dB.

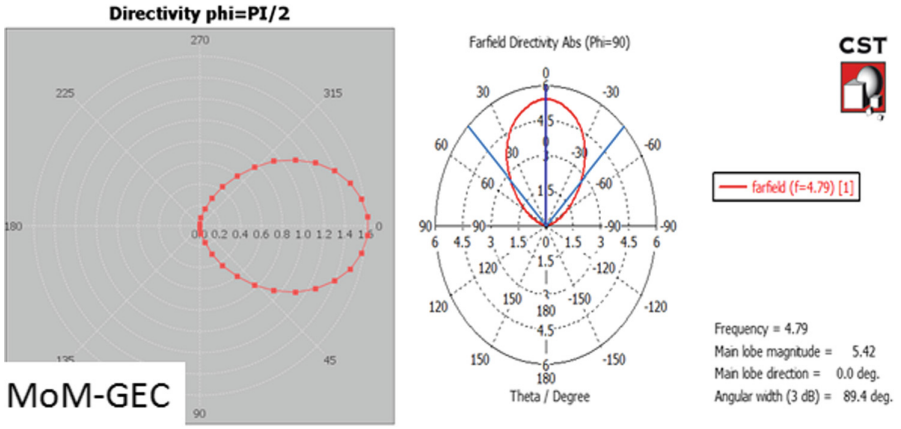

Fig. 7. Directivity along E-plane polar plots (MoM-GEC computation and CST MWS simulation).

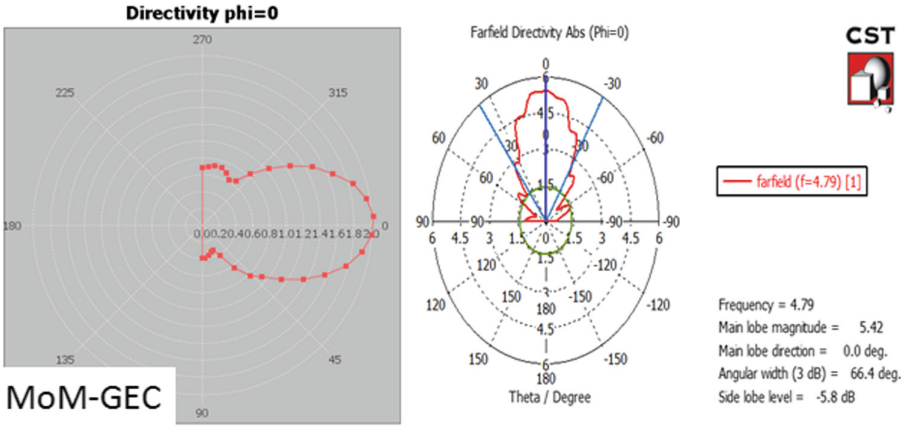

Fig. 8. Directivity along H-plane polar plots (MoM-GEC computation and CST MWS simulation).

5 Conclusion

In this contribution, an investigation of Fraunhofer-zone based on aperture theory is done for planar radiated element contained in open-ended waveguide. The application of aperture antenna theory combined with MoM-GEC analysis is made using Java/Scala computer program. Results described above, show an agreement with both numerical calculation and simulation in terms of radiated field, radiation pattern and directivity. The maximum radiated intensity in the normal direction ($\theta = 0$) to the studied plane is about 5 dB over the rectangular electric aperture. In this paper, we were interested mainly in far-zone, as a future work, our target is to determine radiation properties in the presence of a human body tissue based on Specific Absorption Rate (SAR).

References

1. Zhang, J.H., Wang, J.L.: Maximum power radiated from an aperture antenna before air breakdown in the near-field region. IEEE Trans. Electromagn. Compat. **53**(2), 540–543 (2011)
2. Yaghjian, A.D.: Approximate formulas for the far field and gain of open-ended rectangular waveguide. IEEE Trans. Antennas Propag. **32**(4), 378–384 (1984)
3. Bird, T.S., Lingasamy, V., Selvan, K.T., Sun, H.: Improved finite-range gain formula for openended rectangular waveguides and pyramidal horns. IET Microwaves Antennas Propag. **11**, 2054–2058 (2017)
4. Maheshwari, A., Behera, S., Thiyam, R., Maiti, S., Mukherjee, A.: Near field to Far field Transformation by Asymptotic evaluation of Aperture Radiation field. In: International Conference on Signal Propagation and Computer Technology (ICSPCT) (2014)
5. Lin, Y., Shafai, L.: Moment-method solution of the near field distribution and far field patterns of microstrip antennas. In: IEE Proceedings (1985)
6. Salah, T.B.: Analyse d'une antenne planaire: Utilisation des fonctions d'attache dans la methode des moments. ENIT Tunisia (2003)
7. Harrington, R.F.: Field Computation by Moment-methods. IEEE Antennas and Propagation Society. Wiley (1993)
8. Aubert, H., Baudrand, H.: L'electromagnetisme par les schemas equivalents. Cepadues (2003)
9. Balanis, C.A.: Antenna Theory Analysis and Design, 3rd edn. Wiley-Blackwell (1982)
10. Rengarajan, S.R., Rahmat-Samii, Y.: The field equivalence principle: illustration of the establishment of the non-intuitive null fields. IEEE Antennas Propag. Mag. **42**(4), 122–128 (2000)
11. Sarkar, T.K., Arvas, E.: An integral equation approach to the analysis of finite microstrip antennas: volume/surface formulation. IEEE Trans. Antennas Propag. **38**(3), 305–312 (1990)